

Theoretical and experimental investigations of zone-center optical phonons in wurtzite $\text{Al}_x\text{Ga}_{1-x}\text{N}$ using pseudo unit cell model

M. A. ABID*, H. ABU HASSAN, S. S. NG

Nano-Optoelectronics Research and Technology Laboratory, School of Physics, Universiti Sains Malaysia, 11800 Minden, Penang, Malaysia

Pseudo unit cell (PUC) model was applied to investigate the phonons frequency, mode number, static dielectric constant and high frequency dielectric constant of $\text{Al}_x\text{Ga}_{1-x}\text{N}$ mixed crystals. The theoretical results were compared with experimental results obtained using Raman and Fourier transform infrared spectroscopy on samples with different mole fraction ($0 \leq x \leq 1$) grown on *c*-plane (0001) sapphire substrates. Theoretical results indicated that the $\text{Al}_x\text{Ga}_{1-x}\text{N}$ had only one-mode of vibration for $A_1(\text{LO})$ and classified as two-mode behavior for small Al composition range in agreement with the experimental results which revealed a two-mode behavior for the $E_1(\text{TO})$.

(Received April 06, 2010; accepted May 20, 2010)

Keywords: $\text{Al}_x\text{Ga}_{1-x}\text{N}$, PUC, Phonon, Raman, FTIR, Pseudo unit cell (PUC) model

1. Introduction

The group III-nitride compounds have attracted considerable interest due to their applications for optoelectronic devices, which are active in the blue and ultraviolet spectral regions with high quantum efficiency [1-4]. In particular, their ternaries, $\text{In}_x\text{Ga}_{1-x}\text{N}$ and $\text{Al}_x\text{Ga}_{1-x}\text{N}$, have been extensively studied and found to be useful as well layers and cladding layers in quantum well (QW) laser diode (LD) structures, respectively [5,6]. Phonons play an important role in many of the physical properties of solids, such as the thermal conductivity and the electrical conductivity. Therefore in this paper we investigated the theoretical model of lattice vibrations using pseudo unit cell (PUC) model and compared the results with experimental works done by Raman and FTIR spectroscopy. The purpose of the present work is to study one of the basic physical properties of III-N semiconductors: the optical phonons, especially the optical-phonon-mode behavior in ternary semiconductors. Till now there has been no agreement whether to consider the $\text{Al}_x\text{Ga}_{1-x}\text{N}$ having one-mode or two-mode behavior. Thus this theoretical study by using PUC model and comparison with experiment will provide some answers to this issue. Ternary semiconductors ($A_xB_{1-x}C$) are essential to realizing many physically important parameters necessary to achieve so-called band gap engineering. Generally, optical-phonon characteristics in such ternary semiconductors can be classified into three classes, according to the behavior of their zone-center optical phonons: one-mode, two-mode, and intermediate mode [7]. One-mode behavior exhibits only one set of longitudinal-optical (LO) and transversal-optical (TO) phonons whose frequencies vary almost linearly with compositional changes x . Two-mode behavior exhibits two

sets of phonons for each LO and TO phonon; each set is due to the lighter and heavier component of the two binary semiconductors, i.e., AC and BC; that represent the compositional extremes of the ternary system. The intermediate mode behavior exhibits two-mode behavior for a certain range of composition and one-mode behavior for the remaining compositional range.

2. Phonon theoretical model of the mixed crystal

In the long-wavelength optical lattice vibration theoretical treatment of a ternary mixed crystal $A_xB_{1-x}C$, A and B ions are assumed to be cations and the C ion to be an anion (or vice versa). The theoretical treatment used in this paper is based on the PUC model.

2.1 Pseudo-unit-cell model

The PUC model proposed by Chang and Mitra [8,9] is an excellent theoretical model to investigate the phonon mode, phonon energy and dielectric constant of mixed crystals. This model simplifies greatly the concept of the many-body and random problem of the mixed crystals, and also has the advantage that the Hamiltonian of the mixed system can be obtained directly. By using the PUC model, the electron-phonon interaction in ternary mixed crystals in long-wavelength limit has been obtained [10,11]. The basic assumptions of the PUC model for an $A_xB_{1-x}C$ crystal are as follows [10,12]:

C ions in a rigid sub-lattice (A ions and B ions are in another rigid sub-lattice) are randomly distributed and obeyed the law of statistics. The immediate neighbors of A ions and B ions are always C ions, and the immediate

neighbors of C ions, however, are always A ions or B ions. The probability of finding an A ion as the nearest neighbor of a C ion is equal to the concentration x . The interaction force between the ions consists of two parts; one is a short-range mechanical coupling force and the other is a long-range local electric field force. All elements of the same kind vibrate with the same phase and amplitude (with respect to other different elements). Every atom is under the influence of the interaction force.

2.2 Phonons frequency

The determination of LO phonon frequency, ω_L , and the TO phonon frequency, ω_T , of the ternary $Al_xGa_{1-x}N$ mixed crystal using the PUC model is from the following equations [10]:

$$(1) \begin{vmatrix} b_{11} + m_{11}\omega^2_T & b_{12} + m_{12}\omega^2_T \\ b_{21} + m_{21}\omega^2_T & b_{22} + m_{22}\omega^2_T \end{vmatrix} = 0$$

$$\begin{vmatrix} b'_{11} + m_{11}\omega^2_L & b'_{12} + m_{12}\omega^2_L \\ b'_{21} + m_{21}\omega^2_L & b'_{22} + m_{22}\omega^2_L \end{vmatrix} = 0 \quad (2)$$

where

$$b'_{ij} = b_{ij} - \frac{b_{i3}b_{3j}}{\epsilon_0 + b_{33}}, (i,j=1,2) \quad (3)$$

The coefficients b_{ij} ($i,j=1,2,3$) and m_{ij} ($i,j=1,2,3$) are defined by

$$b_{11} = -x\mu_1\omega^2_{1T} \left[\frac{\epsilon_{10} + 2}{\epsilon_{1\infty} + 2} - x \frac{\epsilon_{10} + \epsilon_{1\infty}}{(\epsilon_{1\infty} + 2)^2} a(x) \right], \quad (4)$$

$$b_{12} = b_{21} = x(1-x)\omega_{1T} \frac{\sqrt{\epsilon_{10} - \epsilon_{1\infty}}}{\epsilon_{1\infty} + 2} \times \omega_{2T} \frac{\sqrt{\epsilon_{20} - \epsilon_{2\infty}}}{\epsilon_{2\infty} + 2} \sqrt{\mu_1\mu_2} a(x), \quad (5)$$

$$b_{13} = x\omega_{1T} \frac{\sqrt{\epsilon_{10} - \epsilon_{1\infty}}}{\epsilon_{1\infty} + 2} \sqrt{\frac{\epsilon_0\mu_1}{n}} a(x), \quad (6)$$

$$b_{22} = -(1-x)\mu_2\omega^2_{2T} \left[\frac{\epsilon_{20} + 2}{\epsilon_{2\infty} + 2} - (1-x) \frac{\epsilon_{20} + \epsilon_{2\infty}}{(\epsilon_{2\infty} + 2)^2} a(x) \right], \quad (7)$$

$$b_{23} = (1-x)\omega_{2T} \frac{\sqrt{\epsilon_{20} - \epsilon_{2\infty}}}{\epsilon_{2\infty} + 2} \sqrt{\frac{\epsilon_0\mu_2}{n}} a(x), \quad (8)$$

$$b_{31} = x\omega_{1T} \frac{\sqrt{\epsilon_{10} - \epsilon_{1\infty}}}{\epsilon_{1\infty} + 2} \sqrt{n\epsilon_0\mu_1} a(x),$$

$$(10) \quad b_{32} = (1-x)\omega_{2T} \frac{\sqrt{\epsilon_{20} - \epsilon_{2\infty}}}{\epsilon_{2\infty} + 2} \sqrt{n\epsilon_0\mu_2} a(x),$$

$$(11) \quad b_{33} = \epsilon_0(a(x) - 3),$$

$$(12) \quad m_{12} = m_{21} = -\frac{xm_A(1-x)m_B}{M},$$

$$m_{11} = \frac{xm_A[(1-x)m_B + m_C]}{M}, \quad (13)$$

$$(14) \quad m_{22} = \frac{(1-x)m_B[xm_A + m_C]}{M},$$

$$(15) \quad \mu_1 = \frac{m_A m_C}{m_A + m_C},$$

$$(16) \quad \mu_2 = \frac{m_B m_C}{m_B + m_C},$$

$$M = xm_A + (1-x)m_B + m_C \quad (17)$$

$$a(x) = 3 \left[1 - x \frac{\epsilon_{1\infty} - 1}{\epsilon_{1\infty} + 2} - (1-x) \frac{\epsilon_{2\infty} - 1}{\epsilon_{2\infty} + 2} \right]^{-1}. \quad (18)$$

where x , μ_1 (μ_2), m_A , m_B and m_C represent the composition, reduce masses of AlN(GaN), and masses of Al, Ga, N atoms, respectively. The terms $\epsilon_{1\infty}$ ($\epsilon_{2\infty}$), ϵ_{10} (ϵ_{20}), ω_{1L} (ω_{2L}) and ω_{1T} (ω_{2T}) are the high frequency dielectric constant, the static dielectric constant, the LO photon frequency and the TO photon frequency of AlN(GaN) binary crystals, respectively. The term n is the number of the total effective masses for the relative coordinate. Wigner-Seitz cells per unit volume and M is by using equations (1) and (2) the LO phonon frequency and the TO phonon frequency of the $Al_xGa_{1-x}N$ are calculated directly from the material parameters of AlN and GaN crystals as given in Table 1.

Table 1. The physical parameters of AlN and GaN crystals used in the (PUC) model [13].

m_A	m_B	m_C	$\varepsilon_{1\infty}$	$\varepsilon_{2\infty}$	$\hbar\omega_{1L}$ (meV)	$\hbar\omega_{2T}$ (meV)	$\hbar\omega_{1L}$ (meV)	$\hbar\omega_{2T}$ (meV)	Lattice constant Å	Lattice constant Å
Al	Ga	N	AlN	GaN	AlN	GaN	AlN	GaN	AlN	GaN
26.982	69.723	14.007	4.84	5.35 ^b	113 ^a	91.8 ^a	83.3	69.3	4.982 ^c	5.185 ^d

^aReference [14,16]^cReference [20]^bReference [15-19]^dReference [15,20]

2.3 Dielectric constant

Important physical parameters required to characterize the optical and electric properties of a crystal are the optical and static dielectric constants, these parameters have a relationship with the refractive index of the crystal. Since the dielectric constants respond to the lattice vibrations, hence we can determine them in the form of phonon theory. The high frequency and static dielectric constants of the $\text{Al}_x\text{Ga}_{1-x}\text{N}$ ternary mixed crystal can be obtained according to the PUC model by [12,21]

$$\varepsilon_{\infty} = 3 \left[1 - x \frac{\varepsilon_{1\infty} - 1}{\varepsilon_{1\infty} + 2} - (1-x) \frac{\varepsilon_{2\infty} - 1}{\varepsilon_{2\infty} + 2} \right]^{-1} - 2 \quad (19)$$

and

$$\varepsilon_0 = \varepsilon_{\infty} \frac{\omega^2_{L_1} \omega^2_{L_2}}{\omega^2_{T_1} \omega^2_{T_2}} \quad (20)$$

where $\omega^2_{L_1}$ and $\omega^2_{L_2}$ ($\omega^2_{T_1}$ and $\omega^2_{T_2}$) are the two LO (TO) phonon frequencies of the ternary mixed crystal. Hence equations (19) and (20) can be used to calculate the static and high frequency dielectric constants theoretically after obtaining the results for phonons frequency from the PUC model.

2.4 Oscillator strength

The oscillator strength is a powerful and useful parameter to judge the characteristic of the phonon modes and provides reasonable explanations of the phonon-mode behavior in the mixed crystal. In the same way for the dielectric constants, we can define the oscillator strengths f_i ($i=1, 2, n$) for phonon modes by the following equation, as introduced by Genzel, Martin, and Perry [21].

$$(21) \varepsilon_0 = \varepsilon_{\infty} + \sum_{i=1}^n \frac{f_i \omega^2_{T_i}}{\omega^2_{T_i}}$$

By comparing equations (20) and (21) and equating it with each other we can find the general equation for the oscillator strength as shown below:

$$f_i = \varepsilon_{\infty} \prod_{j=1}^n (\omega^2_{L_j} - \omega^2_{T_i}) \left[\omega^2_{T_i} \prod_{j=1}^n (\omega^2_{T_j} - \omega^2_{T_i}) \right]^{-1} \quad (22)$$

where \prod denotes the product for all terms excluding ($j=i$).

Equation (22) can be used to calculate the oscillator strength for every optical phonon mode if all of the eigen frequencies of a mixed crystal are known. This equation appears that the phonon oscillator strength f_i will approach to become zero if the frequency of the i th TO phonon mode is very close to any one of the LO-phonon frequencies; on the opposite, f_i will approach to be larger if ω_{T_i} is near any one of the TO-phonon frequencies.

3. Experimental work

The samples used in this study were epilayers of $\text{Al}_x\text{Ga}_{1-x}\text{N}$ ternary nitrides with different mole fraction ($0 \leq x \leq 1$) grown on c -plane (0001) sapphire substrates. Raman and FTIR spectroscopy were performed to measure the optical properties of the samples. The Raman measurements were performed at room temperature using 514.5 nm line from an Ar^+ ion laser as the excitation source. The diameter of the laser spot on the samples was $\sim 1 \mu\text{m}$. The FTIR spectrometer used to perform the IR reflectance of the samples consisted of a potassium bromide (KBr) beam splitter and a mid IR triglycine sulfate (TGS) detector with a resolution of 1 cm^{-1} .

4. Results and discussion

Hexagonal wurtzite (2H) structure of AlN and GaN has four atoms per unit cell [22] leading to an A_1 branch in which the Raman-active phonon is polarized in the c -axis direction and which is infrared active in the extraordinary ray; an E_1 branch in which the phonon polarized in the basal plane can be observed in the infrared in the ordinary ray spectrum, and which is also Raman active; two E_2 branches which are only Raman active; and two silent B_1 modes [23]. The frequency of an optical phonon which is infrared active is split into a longitudinal (LO) and a transverse (TO) component by the macroscopic electric field associated with the relative atomic displacement of the longitudinal phonons. This electric field serves to stiffen the force constant of the phonon and thereby raise the frequency of the (LO) over that of the (TO) [24].

The numerical results for phonon energies, oscillator strengths and dielectric constants of $\text{Al}_x\text{Ga}_{1-x}\text{N}$ ternary mixed crystals using the PUC model are plotted in Fig. 1, Fig. 2 and Fig. 3, respectively. Fig. 1 shows good agreement between theory and experiment for the longitudinal optical phonon $A_1(\text{LO})$ with value as tabulated in Table 2.

Table 2. Optical phonon modes in (cm^{-1}) of $Al_xGa_{1-x}N$ obtained from theory, Raman and polarize IR reflectance measurements.

Sample	Composition x (%)	$A_1(LO)$			$E_1(TO)$		
		Theory	Raman	Polarized IR reflectance	Theory	Polarized IR GaN-like	Polarized IR AlN-like
S1	0	745.2	738.51	739.2	564.0	564.6	-----
S2	5	752.5	767.55	765.4	576.3	568.8	666.2
S3	10	761.1	774.40	771.2	587.3	569.2	668.4
S4	11	762.7	776.35	774.2	589.4	570.0	668.4
S5	13	766.3	777.04	775.0	593.0	570.0	668.4
S6	22	779.9	-----	NA	606.8	571.2	670.4
S7	23	781.4	795.58	794.6	608.1	571.8	672.6
S8	31	792.7	815.46	815.46	618.0	575.4	673.0
S9	33	795.8	814.36	NA	620.4	571.6	676.4
S10	66	836.9	842.02	842.02	650.9	590.2	690.2
S11	100	872.4	889.95	883.4	674.0	-----	675.0

For the transverse optical phonon $E_1(TO)$, there is initially a good agreement to the theory with the GaN-like of the experiment but after that the theoretical $E_1(TO)$ appears in between the two observed $E_1(TO)$ of AlN-like and GaN-like. In the other hand, from Fig. 1, the theoretical $E_1(TO)$ actually represent a mix behavior of the two experimental $E_1(TO)$ from GaN-like to AlN-like, for ($0 < x < 1$). This behavior can be explained by the Fig. 2 of the oscillator strength of mode two which is zero at ($x=1$ and $x=0$) but having small values for ($0 < x < 1$).

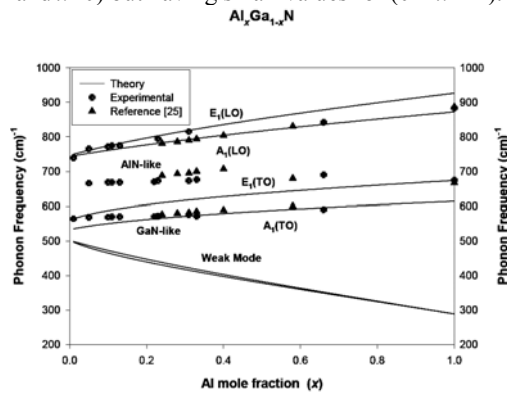


Fig. 1. Phonon frequencies of the $Al_xGa_{1-x}N$ using PUC model in terms of (cm^{-1}).

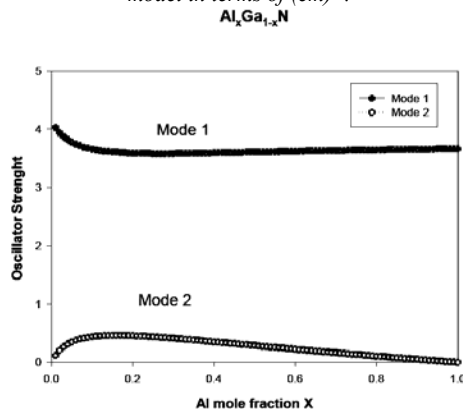


Fig. 2. Oscillator strengths of the $Al_xGa_{1-x}N$ with its mode number by using the PUC model.

Thus, the oscillator strength modeled by PUC is an indicator of the presence of two mode behavior that could be observed in an experimental. This classification is in agreement with our work and with the work of Kazan et al [25]. The phonon mode behavior of $Al_xGa_{1-x}N$ mixed crystals in Fig. 2 is slightly confusing since the oscillator strength of mode two is zero at the two end cases ($x = 0$ and $x = 1$) and increases slightly for small Al composition range, thus $Al_xGa_{1-x}N$ can also be qualitatively classified to one-mode behavior at the end cases ($x = 0$ and $x = 1$) and classified as two-mode behavior in small Al composition range excluding the end value ($x = 0$ and $x = 1$). However, the increase in oscillator strength in this region is very small and do not appear in the theoretical calculation for two mode but has been observed in our FTIR spectrum as shown by the two modes for the $E_1(TO)$ (GaN-like and AlN-like) in Fig. 5.

In Fig. 3, we see that the dielectric constants, ϵ_0 and ϵ_∞ of the ternary $Al_xGa_{1-x}N$, III-nitride mixed crystals decrease with increasing Al mole fraction smoothly and monotonically from one end-member value to the other end-member value over the composition range regardless of the one-or two-mode behavior.

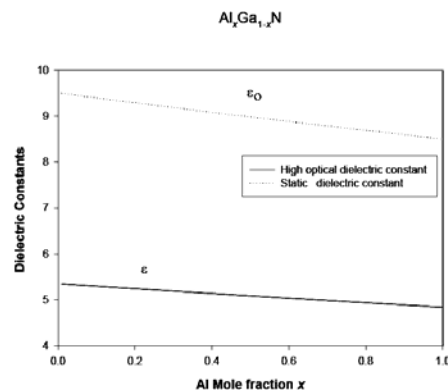


Fig. 3. Static and high frequency dielectric constants of the $Al_xGa_{1-x}N$ by using PUC model.

The Raman spectra in Fig. 4 show that for GaN ($x=0$) sample, all the allowed Raman phonon modes are clearly

visible and are comparable to the reported results [26, 27]. Besides that very weak shoulders corresponding to $E_1(\text{TO})$ mode of GaN-like can also be observed in some of the small Al composition samples. For AlN ($x=1$) sample the Raman spectrum is similar to the case of the GaN sample, which means that all the Raman modes are clearly visible and are in agreement with the reported results [25, 28].

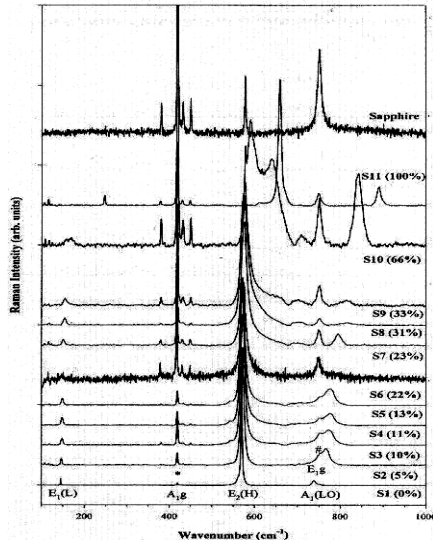


Fig. 4. Room temperature Raman spectra of the $\text{Al}_x\text{Ga}_{1-x}\text{N}$ ($0 \leq x \leq 1$) samples and sapphire substrate.

Infrared reflectance measurement with s- and p-polarization are plotted in Fig. 5 and Fig. 6, respectively. Under these modes, purely transverse optical $E_1(\text{TO})$ and longitudinal optical $A_1(\text{LO})$ phonon modes can be observed for the phonon propagation direction perpendicular and parallel to the crystal axis, respectively. Generally, it can be seen that both sets of the polarization spectra of the $\text{Al}_x\text{Ga}_{1-x}\text{N}$ samples display almost the same patterns and are dominated by Al_2O_3 reststrahlen bands. Nevertheless, the features due to the AlGaN thin films can be distinguished from the pure Al_2O_3 spectra.

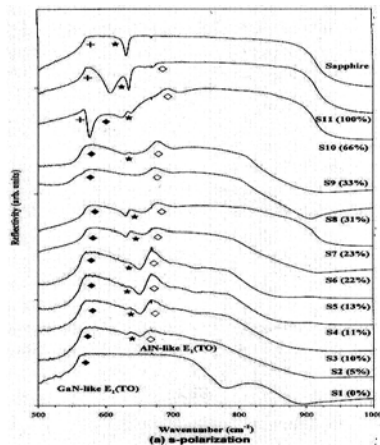


Fig. 5. S-polarization room temperature FTIR spectra of the $\text{Al}_x\text{Ga}_{1-x}\text{N}$ ($0 \leq x \leq 1$) samples and sapphire substrate, close and open diamonds for GaN-like and AlN-like respectively. The stars and crosshairs are the phonon modes for sapphire.

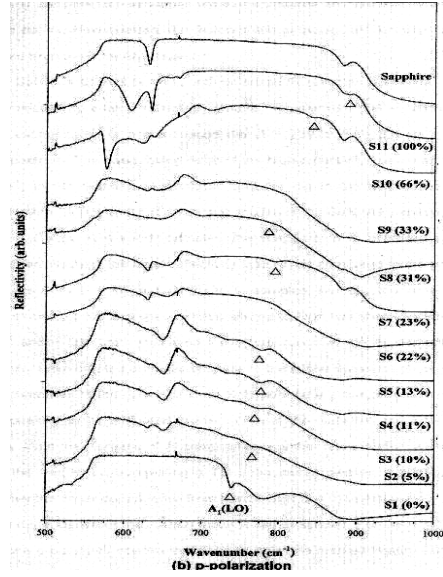


Fig. 6. P-polarization room temperature FTIR spectra of the $\text{Al}_x\text{Ga}_{1-x}\text{N}$ ($0 \leq x \leq 1$) samples and sapphire substrate, the open triangles indicated the $A_1(\text{LO})$ optical mode of the $\text{Al}_x\text{Ga}_{1-x}\text{N}$.

For GaN ($x=0$) (AlN ($x=1$)), both polarized IR reflectance spectra are similar, namely dominated by a large reflectivity feature, namely from $550\text{--}720\text{ cm}^{-1}$ ($650\text{--}850\text{ cm}^{-1}$), except there is a pronounced dip at $\sim 739\text{ cm}^{-1}$ ($\sim 883\text{ cm}^{-1}$) in the p-polarized spectrum. The sharp rising edge of the high reflectivity feature at $\sim 565\text{ cm}^{-1}$ ($\sim 675\text{ cm}^{-1}$) in the s-polarized spectrum and the dip in the p-polarized spectrum correspond to the $E_1(\text{TO})$ and $A_1(\text{LO})$ phonon mode of the GaN (AlN) epilayer, these values are tabulated in Table 2.

For $\text{Al}_x\text{Ga}_{1-x}\text{N}$ ($0 \leq x \leq 1$) samples the shapes of both polarized spectra are different (especially near the large reflectivity feature) as compared to the polarized IR spectra of the GaN ($x=0$) and AlN ($x=1$) samples, namely, the large reflectivity feature in s- and p-polarized spectra have altered to form two sharp peaks centered at $\sim 565\text{ cm}^{-1}$ and $\sim 666\text{ cm}^{-1}$. This indicated that the incorporation of the Al elements into the semiconductor have created dramatic changes to the lattice dynamics of the materials.

5. Conclusions

We have calculated the zone-center optical phonons for ternary nitride semiconductors of $\text{Al}_x\text{Ga}_{1-x}\text{N}$ with different mole fraction ($0 \leq x \leq 1$). Based on a PUC model and the experimental work of FTIR and Raman, it is found that the optical phonon modes in $\text{Al}_x\text{Ga}_{1-x}\text{N}$ exhibit one mode behavior in the theoretical model at the end cases ($x = 0$ and $x = 1$) for $A_1(\text{LO})$ and can be classified as two-mode behavior in small Al composition range excluding the end values ($x = 0$ and $x = 1$) as revealed by the two mode behavior of $E_1(\text{TO})$ in the experimental work.

Acknowledgments

Financial supports from Science Fund, Ministry of Science, Technology and Innovation (MOSTI) and Universiti Sains Malaysia are gratefully acknowledged.

References

- [1] E. L. Piner, F. G. McIntosh, J. C. Roberts, M. E. Aumer, V. A. Joshkin, S. M. Bedair, N. A. El-Masry, *MRS Internet J. Nitride Semicond. Res.* **1**, 43 (1996).
- [2] H. Hirayama, A. Kinoshita, T. Yamabi, Y. Enomoto, A. Hirata, T. Araki, Y. Nanishi, Y. Aoyagi, *Appl. Phys. Lett.* **80**, 207 (2002).
- [3] J. Zhang, J. Yang, G. Simin, M. Shatalov, M. Asif Khan, M. S. Shur, R. Gaska, *Appl. Phys. Lett.* **77**, 2668 (2000).
- [4] C. Marinelli, M. Bordovsky, L. J. Sargent, M. Gioannini, J. M. Rorison, R. V. Penty, I. H. White, P. J. Heard, M. Benyoucef, M. Kuball, G. Hasnain, T. Takeuchi, R. P. Schneider, *Appl. Phys. Lett.* **79**, 4076 (2001).
- [5] I. Akasaki, S. Sota, H. Sakai, T. Tanaka, M. Koike, H. Amano, *Electron. Lett.* **32**, 1105 (1996).
- [6] N. Yamada, Y. Kaneko, S. Watanabe, Y. Yamaoka, T. Hidaka, S. Nakagawa, E. Marenger, T. Takeuchi, S. Yamaguchi, H. Amano, I. Akasaki, 10th IEEE/Lasers and Electro-Optics Society Annual Meet. PD1.2, 1997.
- [7] I. F. Chang and S. S. Mitra, *Adv. Phys.* **20**, 359 (1971).
- [8] I. F. Chang, Ph.D. dissertation, University of Rhode Island, 1968.
- [9] I. F. Chang, S. S. Mitra, *Phys. Rev.* **172**, 924 (1968).
- [10] R. S. Zheng, M. Matsuura, *Phys. Rev. B* **59**, 15422 (1999).
- [11] R. S. Zheng, T. Taguchi, M. Matsuura, *J. Appl. Phys.* **87**, 2526 (2000).
- [12] R. S. Zheng, T. Taguchi, M. Matsuura, *Phys. Rev. B* **66**, 075327 (2002).
- [13] V. Bougrov, M. E. Levinstein, S. L. Romyantsev, A. Zubrilov, in *Properties of Advanced Semiconductor Materials GaN, AlN, InN, BN, SiC, SiGe*, Eds. M. E. Levinstein, S. L. Romyantsev, M. S. Shur, John Wiley & Sons, Inc., New York, 1, 2001.
- [14] V. Yu. Davydov, Yu. E. Kitaev, I. N. Goncharuk, A. N. Smirnov, J. Graul, O. Semchinova, D. Uffmann, M. B. Smirnov, A. P. Mirgorodsky, R. A. Evarestov, *Phys. Rev. B*, **58**, 12899 (1998).
- [15] H. Harima, *Journal of Physics :Cond .Matter* **14**, R967 (2002).
- [16] R.,S Goldhan, Shokhovets, in *III-nitride semiconductors optical properties II*, M. O. Manasreh, H. X. Jiang, editors, Taylor&Francis **73** 63 (2002).
- [17] S. N. Mohammad, H. Morcoc, *Prog. Quant.EI.* **20**, 361 (1996).
- [18] Monemar, J. *Material Sci.:Materials in Electronics*.**10**, 227 (1999).
- [19] R. Goldhan, S. Shokhovets, in *III-nitride semiconductors optical properties II*, M. O. Manasreh, H. X. Jiang, editors, Taylor&Francis **73**, 63 (2002).
- [20] I. Vurgaftman, J. R. Meyer, L. R. Ram-Mohan, *J. Appl. Phys.* **89**, 5815 (2001).
- [21] L. Genzel, T. P. Martin, C. H. Perry, *Phy. Status Solidi B* **62**, 83 (1974).
- [22] R. Loudon, *Adv. Phys.* **13**, 423 (1964).
- [23] M. Tinkham, *Group Theory and Quantum Mechanics*, McGraw-Hill, New York, 1964.
- [24] Leah Bergman, Mitra Dutta, Cengiz Balkas, Robert F. Davis, James A. Christman, Dimitri Alexson, Robert J. Nemanich, *J. Appl. Phys.* **85**, 3535 (1999).
- [25] M. Kazan, P. Masri, M. Sumiya, *J. Appl. Phys.* **100**, 013508 (2006).
- [26] U. Haboek, H. Siegle, A. Hoffmann, C. Thomsen, *Phys. Stat. Sol. (C)*, 1710 (2003) .
- [27] Harima, H. J. *Phys.:Condens.Matter* **14**, R967 (2002).
- [28] M. Beshkova, Z. Zakhariev, M. V. Abrashev, E. Birch, A. Kakanakova, R. Yakimova, *Vacuum* **76**, 143 (2004).

*Corresponding author: muslim_abid@yahoo.com